

# Constraints on the C K M angle from the measured C P asymmetries and branching ratios of $B \rightarrow \pi^+ \pi^-$ ; $B \rightarrow \pi^0 \pi^0$ and $K \rightarrow \pi^0 \pi^0$ decays

Zhenjun Xiao

Department of Physics, Nanjing Normal University, Nanjing, Jiangsu 210097, P. R. China  
Caidian Lu<sup>y</sup>

CCAST (World Laboratory), P. O. Box 8730, Beijing 100080, P. R. China;  
and

Institute of High Energy Physics, P. O. Box 918 (4), Beijing 100039, P. R. China<sup>z</sup>  
Libo Guo

Department of Physics, Nanjing Normal University, Nanjing, Jiangsu 210097, P. R. China  
(April 15, 2024)

## Abstract

In this paper, we draw constraints on the Cabibbo-Kobayashi-Maskawa (CKM) angle and the strong phase from the experimental measurements of  $\sin(2\beta)$ , the CP-violating asymmetries and branching ratios of  $B \rightarrow \pi^+ \pi^-$ ;  $B \rightarrow \pi^0 \pi^0$  and  $K \rightarrow \pi^0 \pi^0$  decays. In the SM, the measured  $\sin(2\beta)$  leads to an upper limit on  $\beta$ :  $\beta < 180^\circ$ . Taking the weighted-average of the newest BaBar and Belle measurements of  $S$  and  $A$  in  $B \rightarrow \pi^+ \pi^-$  decay as the experimental input, we find the allowed range of angle  $\beta$ ,  $76^\circ < \beta < 135^\circ$  for  $r = \mathcal{P}/\mathcal{T} = 0.3 \pm 0.1$ . From the measured CP-averaged branching ratios of  $B \rightarrow \pi^+ \pi^-$ ;  $B \rightarrow \pi^0 \pi^0$  and  $K \rightarrow \pi^0 \pi^0$  decays, we found an inequality,  $\cos \delta \cos \phi > 0.45$ . The region of  $70^\circ < \beta < 110^\circ$  is thus excluded by applying this inequality. The combined constraints on  $\beta$  and  $\delta$  are  $117^\circ < \beta < 135^\circ$  and  $160^\circ < \delta < 132^\circ$  if we take  $S = 0.49 \pm 0.27$  and  $A = 0.51 \pm 0.19$  as the experimental input. The new lower limit on the angle  $\beta$  is dominated by the measured branching ratios considered in this paper, and is much stronger than those obtained before.

Typeset using REVTeX

---

Email address: zjxiao@em ailn jnu .edu.cn

<sup>y</sup>Email address: lucd@ ih ep .ac.cn

<sup>z</sup>Mailing address.

## I. INTRODUCTION

To measure the Cabibbo-Kobayashi-Maskawa (CKM) angles  $\alpha$ ,  $\beta$  and  $\gamma$  is one of the main goals of the B factory experiments. In the standard model (SM), the CP violation is induced by the nonzero phase angle appeared in the CKM mixing matrix  $V_{CKM}$ , and the unitarity of the matrix  $V_{CKM}$  leads to the constraint

$$\alpha + \beta + \gamma = 180^\circ : \quad (1)$$

Recent measurements of  $\sin 2\beta$  in neutral B meson decay  $B_d^0 \rightarrow J/\psi K_{S,L}^0$  by BaBar [1,2] and Belle [3,4] Collaborations established the third type CP violation (interference between the decay and mixing) of  $B_d$  meson system. The world average of  $\sin(2\beta)$  dominated by the newest BaBar and Belle measurements [2,4] is [5]

$$\sin(2\beta) = 0.734 \pm 0.054; \quad (2)$$

which leads to a twofold solution of the angle  $\beta$ :

$$\beta = 23.6^{+2.4}_{-2.2}^\circ \quad \text{or} \quad 66.4^{+2.2}_{-2.4}^\circ : \quad (3)$$

The first solution is in perfect agreement with the global fit results as given for example in Refs. [6-8], while the second one cannot be explained in the SM and requires the existence of new physics [9]. Several strategies to distinguish these two solutions through a measurement of the sign of  $\cos 2\beta$  have been proposed [10] recently. In this paper, we will use the first solution of the angle  $\beta$  as the experimental input.

After the experimental measurement of the angle  $\beta$ , more attention has turned to ways of learning the angle  $\alpha$  and  $\gamma$ . For the determination of the angle  $\alpha$ , the measured CP-averaged branching ratios of  $B \rightarrow K^* \pi$  decays play a key role, and have been studied intensively in the literature [11-14]. But the direct constraint from experiments on  $\alpha$  is still weak.

The CKM angle  $\gamma$  (or  $\alpha_2$  in Belle's word) can be determined by the experimental measurements for the CP violating asymmetries of  $B_d^0 \rightarrow \pi^+ \pi^-$  decays [9,15-17]. From the experimental measurements of the branching ratios of  $B \rightarrow \pi \pi$  and  $K \pi$  decays, one can also extract out the CKM angle  $\gamma$  [15,18,19]. Very recently, based on the data sample of about 85 and 88 million  $(4S) \rightarrow B^+ B^-$  decays, BaBar and Belle collaboration reported their measurements of the CP violation of the  $B_d^0 \rightarrow \pi^+ \pi^-$  decay [20,21], respectively. BaBar result [20]:

$$\begin{aligned} S &= 0.02 \pm 0.34 (\text{stat.}) \pm 0.05 (\text{syst.}); \\ C &= -0.30 \pm 0.25 (\text{stat.}) \pm 0.04 (\text{syst.}); \end{aligned} \quad (4)$$

and Belle [21]:

$$\begin{aligned} S &= -1.23 \pm 0.41 (\text{stat.})^{+0.08}_{-0.07} (\text{syst.}); \\ A &= +0.77 \pm 0.27 (\text{stat.}) \pm 0.08 (\text{syst.}); \end{aligned} \quad (5)$$

It is easy to see that the experimental measurements of the BaBar and Belle collaboration are not fully consistent with each other: BaBar's result is still consistent with zero, while

the Belle's result strongly indicate nonzero  $S$  and  $A$ . But we do believe that the current discrepancy between two collaborations will disappear when more data become available. If we make a weighted average<sup>1</sup> of the two experiments, and find that

$$S = 0.49 \pm 0.27(0.61); \quad (6)$$

$$A = +0.51 \pm 0.19(0.23); \quad (7)$$

where the errors in brackets are those increased by the PDG scaling-factor procedure [23].

In a previous paper [17], based on the data as reported by BaBar and Belle Collaboration [20,22], we presented the general description of CP asymmetries of the  $B \rightarrow \pi^+ \pi^-$  decay and found the constraint on the CKM angle  $\alpha$  and the strong phase  $\delta$ .

In this paper, in order to refine the constraints on both  $\alpha$  and  $\delta$ , we will focus on the following experimental information: (a) the new measurements of CP-violating asymmetries of  $B \rightarrow \pi^+ \pi^-$  [20,21]; (b) the wellmeasured CP-averaged branching ratios of  $B \rightarrow \pi^+ \pi^-$ ;  $B \rightarrow \pi^0 \pi^0$  and  $K^0 \pi^+$  decays [24-26]; and (c) the world average of  $\sin(2\beta)$  as given in Eq.(2) [5]. For the sake of completeness and comparison, we also quote the constraints on the CKM angles from global fit [6-8].

This paper is organized as follows. In Sec. II, we give a brief review about the definition of the CKM angles, draw direct constraint on the CKM angle  $\alpha$  from the measured  $\sin(2\beta)$ . In Sec. III we present the general description of CP asymmetries of the  $B \rightarrow \pi^+ \pi^-$  decay, consider new BaBar and Belle's measurements of  $S$  and  $A$  to draw the constraints on the CKM angle  $\alpha$  and the strong phase  $\delta$ . In Sec. IV we take the wellmeasured branching ratios of  $B \rightarrow \pi^+ \pi^-$ ;  $B \rightarrow \pi^0 \pi^0$  and  $K^0 \pi^+$  decay modes into account, estimate the ratio of tree to penguin amplitude  $|T/P|$ , and finally draw the constraints on both the CKM angle  $\alpha$  and the strong phase  $\delta$ . The conclusions are included in the final section.

## II. THE CKM ANGLES $\alpha$ , $\beta$ AND $\gamma$ IN THE SM

In the SM with  $SU(2) \times U(1)$  as the gauge group, the quark mass eigenstates are not the same as the weak eigenstates. The mixing between the down type quark mass eigenstates was described by a  $3 \times 3$  unitary matrix  $V_{CKM}$  [27]. The elements of the CKM matrix  $V_{CKM}$  are fixed by four parameters, one of which is an irreducible complex phase. Using the generalized Wolfenstein parametrization [28],  $V_{CKM}$  can be written as

$$V_{CKM} = \begin{pmatrix} 1 - \frac{\lambda^2}{2} & A \lambda^3 (1 - i) & A \lambda^2 \\ -A \lambda^3 (1 - i) & 1 - \frac{\lambda^2}{2} & A \lambda^2 \\ A \lambda^3 & -A \lambda^2 & 1 \end{pmatrix} \quad (8)$$

where  $\lambda = \sin(\theta/2)$ ,  $\theta = (1 - \lambda^2/2)$ , and  $A$ ,  $\rho$ , and  $\phi$  are the four independent Wolfenstein parameters. The parameter  $A$  and  $\phi$  have been measured with good precision,

$$|V_{us}| = 0.2196 \pm 0.0026 \quad (9)$$

---

<sup>1</sup>For the parameter  $A$  and  $C$ , there is a sign difference between the conventions of Belle and BaBar Collaboration:  $A = -C$ . We here use Belle's convention [22].

from analysis of  $K_{e3}$  decays [23], and

$$A = \frac{J_{\text{abj}}}{2} = 0.854 \pm 0.042 \quad (10)$$

determined from the measured  $\dot{V}_{\text{cb}} = (41.2 \pm 2.0) \times 10^3$  and  $\sigma = 0.2196 \pm 0.0026$  [23].

The unitarity of the CKM matrix implies six "unitarity triangle". One of them corresponding to the  $b \rightarrow d$  transition yields

$$V_{ud}V_{ub} + V_{cd}V_{cb} + V_{td}V_{tb} = 0: \quad (11)$$

This unitarity triangle (UT) is just a geometrical presentation of this equation in the complex plane, as illustrated in Fig.1. The three CKM angles in Fig.1 are defined as

$$= \arg \frac{V_{tb} V_{td}}{V_{ub} V_{ud}} ; \quad (12)$$

$$= \arg \frac{V_{cb}V_{cd}}{V_{tb}V_{td}}; \quad (13)$$

$$= \arg \frac{V_{ub}V_{ud}}{V_{cb}V_{cd}} : \quad (14)$$

These definitions are independent of any kind of parametrization of the CKM matrix elements, and therefore universal. In the rescaled UT,  $R_b$  and  $R_t$  denote the lengths of the two sides as shown in Fig. 1, and have been defined as

$$R_b \frac{j_{ud} V_{ub}}{j_{cd} V_{cb}} = \frac{q}{2 + \frac{1}{2}} = (1 - \frac{1}{2}) \frac{V_{ub}}{V_{cb}}; \quad (15)$$

$$R_t \frac{J_{td} V_{tb} j}{J_{cd} V_{cb} j} = \frac{q}{(1 - \eta)^2 + \eta^2} = \frac{1}{\eta} \frac{V_{td}}{V_{cb}} : \quad (16)$$

In terms of  $(\vec{r}; \vec{p})$ ,  $\sin(2\vec{p})$  ( $\vec{p} = \vec{r}; \vec{p}$ ) can be written as

$$\sin(2\theta) = \frac{2(\sigma^2 + \tau^2)}{(\sigma^2 + \tau^2)((1-\sigma^2)^2 + \tau^2)}; \quad (17)$$

$$\sin(2\theta) = \frac{2(1-\alpha)}{(1-\alpha)^2 + \frac{1}{2}}; \quad (18)$$

$$\sin(2\theta) = \frac{2}{2 + \sqrt{2}} : \quad (19)$$

Within the framework of the SM, intensive studies have been done to constrain the UT by a global fit using the currently available data on neutral K, B mixing, semi-leptonic B and K meson decays [6,8], such as  $V_{us}$ ,  $V_{cb}$ ,  $V_{ub}$ ,  $V_{td}$ ,  $V_{ts}$ , and  $\sin(2\beta)$ . The constraint in the  $(\rho, \eta)$  plane resulting from Eq. (15), for example, is represented by a circle of radius  $R_b$  that is centered at  $(\rho, \eta) = (0,0)$ , while the measured  $\alpha$  may fix a hyperbola in the  $(\rho, \eta)$  plane. The commonly allowed region for the apex of the UT in the  $(\rho, \eta)$  plane corresponds to the so-called global fit result. The ranges for the CKM angles  $\beta$ ,  $\gamma$ , and  $\delta$  obtained by a recent CKM fit are [6]

$$80^\circ < \alpha < 126^\circ; 14^\circ < \beta < 27^\circ; 34^\circ < \gamma < 82^\circ; \quad (20)$$

And the new global fit results can be found in Ref. [8], the typical ranges for the CKM angles are [29]

$$70^\circ < \alpha < 130^\circ; 20^\circ < \beta < 30^\circ; 50^\circ < \gamma < 70^\circ; \quad (21)$$

It is easy to see that the indirect constraint on the angle  $\alpha$  agrees very well with the first solution  $\alpha = (23.6^{+2.4}_{-2.2})^\circ$  in Eq.(3) from the BaBar and Belle's measurements, but strongly disfavor the second solution  $\alpha = 66^\circ$ . We therefore take  $\alpha = 23.6^\circ$  as the physical solution in our analysis and treat the limit

$$180^\circ - \alpha = 156.4^\circ \quad (22)$$

as the direct physical upper limit on the angle  $\alpha$ .

It is worth to mention that the constraints on the CKM angles from global analysis also depend on the specific statistical method used in the analysis (for example, the Bayesian, R<sup>2</sup>, or Scanning method, etc.), but the resulted difference is not significant. For more details about the global fit of the UT parameters, one can see the new CERN Report [8] and references therein.

### III. CP ASYMMETRIES OF $B \rightarrow \pi^+ \pi^-$ DECAY

The  $B \rightarrow \pi^+ \pi^-$  decay mode plays an important role in measuring the angle  $\alpha$ . As shown in Fig.2, both the tree and penguin diagrams contribute to the  $B \rightarrow \pi^+ \pi^-$  decay simultaneously. The tree (T) contribution comes from  $b \rightarrow u \bar{u} d$  transition by exchanging a W boson, while there are QCD penguin (P) and color-suppressed electroweak penguin ( $P_{EW}^C$ ) contributions with internal quarks  $q = (u; c; t)$ . The suppressed annihilation diagrams have been neglected.

#### A. Parametrization of $B \rightarrow \pi^+ \pi^-$ decay

From Fig.2, the decay amplitude  $A(B_d^0 \rightarrow \pi^+ \pi^-)$  and its conjugate  $A(B_d^0 \rightarrow \pi^- \pi^+)$  can be written as [31]

$$A(B_d^0 \rightarrow \pi^+ \pi^-) = [V_{ub}V_{ud}T + V_{tb}V_{td}P_t + V_{cb}V_{cd}P_c + V_{ub}V_{ud}P_u]; \quad (23)$$

$$A(B_d^0 \rightarrow \pi^- \pi^+) = [V_{ub}V_{ud}T + V_{tb}V_{td}P_t + V_{cb}V_{cd}P_c + V_{ub}V_{ud}P_u]; \quad (24)$$

where T is the tree amplitude, and  $P_i$  ( $i = u; c; t$ ) are penguin amplitudes. Using the CKM unitarity relation as given in Eq.(11), the decay amplitude A can be rewritten in three different ways<sup>2</sup> [36]

---

<sup>2</sup>This is the so-called CKM ambiguity [30].

$$\text{Convention A : } A = [V_{ub}V_{ud}T_{uc} + V_{tb}V_{td}P_{tc}]; \quad (25)$$

$$\text{Convention B : } A = [V_{ub}V_{ud}T_{ut} - V_{cb}V_{cd}P_{tc}]; \quad (26)$$

$$\text{Convention C : } A = [V_{tb}V_{td}T_{ut} - V_{cb}V_{cd}T_{uc}]; \quad (27)$$

with

$$T_{ut} = T + P_u - P_t; \quad T_{uc} = T + P_u - P_c; \quad (28)$$

$$P_{tc} = P_t - P_c; \quad (29)$$

The first two conventions are frequently used in previous studies [15{17,19], the third one is also considered in Ref. [36].

In our analysis, we use Convention A and write the amplitudes  $A$  and  $A$  in the following way

$$A = [V_{ub}V_{ud}T_{uc} + V_{tb}V_{td}P_{tc}] = e^{i\phi_T} e^{i\phi_P} [T + P_u - P_t]; \quad (30)$$

$$A = [V_{ub}V_{ud}T_{uc} + V_{tb}V_{td}P_{tc}] = e^{i\phi_T} e^{i\phi_P} [T + P_u - P_t]; \quad (31)$$

The SM predicts the CP-violating asymmetries in the time-dependent rates for initial  $B^0$  and  $B^0$  decays to a common CP eigenstate  $f_{CP}$ . In the case of  $f_{CP} = \pi^+$ , the time-dependent rate is given by

$$\Gamma(B^0(t)) = \frac{e^{-\Gamma t}}{4\Gamma_{B^0}} [1 + q |S| \sin(\Delta m_d t) + A \cos(\Delta m_d t)]; \quad (32)$$

where  $\Gamma_{B^0}$  is the  $B^0$  lifetime,  $\Delta m_d$  is the mass difference between the two  $B^0$  mass eigenstates,  $t = t_{CP} - t_{tag}$  is the time difference between the tagged- $B^0$  ( $B^0$ ) and the accompanying  $B^0$  ( $B^0$ ) with opposite flavor decaying to  $\pi^+$  at the time  $t_{CP}$ ,  $q = +1$  ( $-1$ ) when the tagging  $B$  meson is a  $B^0$  ( $B^0$ ). The CP-violating asymmetries  $S$  and  $A$  have been defined as

$$S = \frac{2\text{Im}(\gamma)}{1 + |\gamma|^2}; \quad A = \frac{1 - |\gamma|^2}{1 + |\gamma|^2}; \quad (33)$$

where the parameter  $\gamma$  is of the form

$$\gamma = \frac{qA}{pA} = e^{2i\phi} \frac{1 - re^{i(\phi_T - \phi_P)}}{1 + re^{i(\phi_T - \phi_P)}}; \quad (34)$$

where  $\phi = \phi_P - \phi_T$  is the difference of CP conserving strong phases, while the ratio of penguin to tree amplitudes of the  $B \rightarrow \pi^+$  decay takes the form

$$r = \frac{P}{T} = \frac{V_{tb}V_{td}P_{tc}}{V_{ub}V_{ud}T_{uc}}; \quad (35)$$

based on the definition of decay amplitudes in Eqs. (25,30). By explicit calculations, we find that<sup>3</sup>

---

<sup>3</sup>By a transformation of  $\gamma \rightarrow \gamma^*$ , the expressions of  $S$  and  $A$  here will become identical with those in Ref. [17].

$$S = \frac{\sin 2\alpha + 2r \cos \alpha \sin \alpha}{1 + r^2 + 2r \cos \alpha \sin \alpha}; \quad (36)$$

$$A = \frac{2r \sin \alpha \sin \alpha}{1 + r^2 + 2r \cos \alpha \sin \alpha}; \quad (37)$$

By setting  $r = 0$ , one would find

$$A = 0; S = \sin(2\alpha); \quad (38)$$

which clearly means that one can measure the  $\sin(2\alpha)$  directly from  $B_d^0 \rightarrow \pi^+ \pi^-$  decay in case of neglecting the penguin contribution to this decay. This is the reason why  $B_d^0 \rightarrow \pi^+ \pi^-$  decay was assumed to be the best channel to measure CKM angle  $\alpha$  previously. But the measurements of  $B \rightarrow \pi \pi$  and  $K \rightarrow \pi \pi$  decays show that the penguin contribution should be rather large. With penguin contributions, we have  $A \neq 0$  and  $S \neq \sin(2\alpha)$ . Besides the Eq.(36),  $S$  can also be defined as [18]

$$S = \frac{1}{1 - A^2} \sin(2\alpha_{\text{eff}}); \quad (39)$$

or

$$S = \sin(2\alpha_{\text{eff}}); \quad (40)$$

Here the allowed range of  $\alpha_{\text{eff}}$  can be determined by the measurements of  $S$  and  $A$  directly. The key problem is how to determine the differences

$$\alpha - \alpha_{\text{eff}}; \quad \alpha - \alpha_{\text{eff}}; \quad (41)$$

which depends on the magnitude and strong phases of the tree and penguin amplitudes. In this case, the CP asymmetries can not tell the size of angle  $\alpha$  directly. A method has been proposed to extract CKM angle  $\alpha$  using  $B^+ \rightarrow \pi^+ \pi^0$  and  $B^0 \rightarrow \pi^0 \pi^0$  decays together with  $B_d^0 \rightarrow \pi^+ \pi^-$  decay by the isospin relation [33]. However, it will take quite some time for the experiments to measure the three channels together. In Ref. [18], Charles studied the ways to estimate  $\alpha$  from the measured branching ratios of  $B \rightarrow \pi \pi$  and  $B \rightarrow \pi K$  decays. In next section, we will extract the constraints on both  $\alpha$  and  $\alpha_{\text{eff}}$  directly by considering the latest experimental measurements about the relevant branching ratios of  $B \rightarrow \pi^+ \pi^-; \pi^+ \pi^0$  and  $K \rightarrow \pi^+ \pi^-$  decays.

#### B. Estimation of the ratio $r = \mathcal{P} = T/j$

From Eqs.(36,37), one can see that the asymmetry parameter  $S$  and  $A$  generally depend on only three "free" parameters: the CKM angle  $\alpha$ , the strong phase  $\delta$  and the ratio  $r$ . We can not solve out these two equations with three unknown variables directly. However, we can find definite constraint on the angle  $\alpha$  and strong phase  $\delta$  if the ratio  $r = \mathcal{P} = T/j$  can be determined experimentally, or at least estimated theoretically with good precision.

Up to now, many attempts have been made to estimate the ratio  $r$  in various ways [15,18,19,33,32,34,35]. Three typical estimations of  $r$  are the following.

In Ref. [35], Beneke et al. made a theoretical estimation of the ratio  $r$ . Employing the QCD factorization approach and neglecting the annihilation amplitude, the  $B \rightarrow \pi^+$  decay amplitude can be written as [35]

$$\begin{aligned} A(B \rightarrow \pi^+) &= V_{ub}V_{ud} \left[ a_1^h + a_4^u + a_{10}^u + r(a_6^u + a_8^u) \right] A \\ &\quad + V_{cb}V_{cd} \left[ a_4^c + a_{10}^c + r(a_6^c + a_8^c) \right] A \\ &\quad + V_{ub}V_{ud}b_1 + (V_{ub}V_{ud} + V_{cb}V_{cd})b_3 + 2b_4 \left[ \frac{1}{2}b_3^{EW} + \frac{1}{2}b_4^{EW} \right] B \end{aligned} \quad (42)$$

with

$$A = \frac{G_F}{\sqrt{2}} (m_B^2 - m^2) F_0^{B \rightarrow \pi} (m^2) f; \quad (43)$$

$$B = \frac{G_F}{\sqrt{2}} f_B f^2; \quad (44)$$

where the coefficients  $a_1$  and  $a_2$  describe the tree diagram contribution,  $a_i^u$  and  $a_i^c$  describe the QCD penguin (for  $i=4,6$ ) and electroweak penguin (for  $i=8,10$ ) contributions induced by the penguin diagrams with internal up or charm quark respectively, the coefficients  $b_i$  describe the weak annihilation contributions [35], and  $f_B$  and  $f$  are the  $B$  and  $\pi$  meson decay constants,  $F_0^{B \rightarrow \pi}$  is the form factor of  $B \rightarrow \pi$  transition, and the factor  $r$  describes the so-called chiral-enhancement [35] to  $B \rightarrow \pi^+$  decay. The explicit expressions of  $a_i$  can be found in Ref. [35].

In Ref. [35], the "tree" and "penguin" part of decay amplitude (42) were defined as the amplitude proportional to the CKM factor  $V_{ub}V_{ud}$  and  $V_{cb}V_{cd}$  respectively (i.e. using the convention B), and the ratio took the form [35]

$$\frac{P}{T} = \frac{V_{cb}V_{cd}}{V_{ub}V_{ud}} \frac{a_4^c + a_{10}^c + r(a_6^c + a_8^c) + r_A \left[ b_3 + 2b_4 \left( \frac{1}{2}b_3^{EW} + \frac{1}{2}b_4^{EW} \right) \right]}{a_1^h + a_4^u + a_{10}^u + r(a_6^u + a_8^u) + r_A \left[ b_1 + b_3 + 2b_4 \left( \frac{1}{2}b_3^{EW} + \frac{1}{2}b_4^{EW} \right) \right]} \quad (45)$$

where  $r_A = B \rightarrow A = 0.003$ . The corresponding numerical result was [35]

$$r = \frac{P}{T} = 0.285 \pm 0.076 \pm (0.259 \pm 0.068); \quad (46)$$

when the weak annihilation contributions are included or not.

The magnitude of the ratio  $r$  can also be estimated by considering the measured branching ratios for the tree dominated  $B \rightarrow \pi^+ \pi^0$  decay and the pure penguin channel  $B \rightarrow K^0 \pi^+$ . But because of the unitarity relation of the CKM matrix, one can define the tree and penguin amplitude in different ways, i.e. choose different convention in one's calculation. For  $B \rightarrow \pi^+ \pi^0$  decay, there are three different conventions, as defined in Eqs.(25-27). For  $B \rightarrow \pi^+ \pi^0$  and  $K^0 \pi^+$  decay modes, we meet the similar situation.

The first convention considered here is the Luo and Rosner (LR) convention. In Ref. [19], Luo and Rosner defined the strangeness-preserving  $b \rightarrow d$  penguin amplitude  $P$  in the  $B \rightarrow \pi^+ \pi^0$  decay as the amplitudes proportional to the CKM combination  $V_{td}V_{tb}$  (i.e. the convention A as given in Eq.(25)), while set the  $b \rightarrow s$  penguin amplitude  $P_K$  in the



pure penguin  $B^+ \rightarrow K^{*0} \pi^+$  decay as the amplitudes proportional to  $V_{ts}V_{tb}$ . By quoting all decay rates in units of  $B$  branching ratio  $10^6$ ) and using the world average available at that time [19], they found that

$$B(B^+ \rightarrow K^{*0} \pi^+) = \frac{1}{\mathcal{P}_K} \mathcal{P}_{\pi^+} = 17.2 \pm 2.4; \quad (47)$$

which leads to

$$\mathcal{P}_{\pi^+} = 4.02 \pm 0.28; \quad (48)$$

and

$$\mathcal{P}_{\pi^+} = \frac{V_{td}}{V_{ts}} \mathcal{P}_{\pi^+} = 0.71 \pm 0.14; \quad (49)$$

By using the theoretical estimation of the form factor shapes and the measurement of the spectrum of  $B \rightarrow \pi$  near  $q^2 = 0$  where  $q^2$  is the squared effective mass of the  $\pi$  system, Luo and Rosner [19] estimated the "tree" part of the  $B \rightarrow \pi^+ \pi^-$  decay rate and then obtained the value of the parameter  $T$

$$T = 2.7 \pm 0.6; \quad (50)$$

which leads to

$$r = \frac{P}{T} = 0.26 \pm 0.08; \quad (51)$$

The second convention considered here is the Gronau and Rosner (GR) convention. In Ref. [15], Gronau and Rosner defined the penguin amplitude  $P$  of  $B \rightarrow \pi^+ \pi^-$  decay as the amplitude proportional to the CKM combination  $V_{cd}V_{cb}$  (i.e. the convention  $B$  as given in Eq.(26)), and set the  $b \rightarrow s$  penguin amplitude  $P_K$  in the pure penguin  $B^+ \rightarrow K^{*0} \pi^+$  decay as the amplitude proportional to  $V_{cs}V_{cb}$ , they then found numerically that

$$\mathcal{P}_{\pi^+} = \frac{V_{cd}V_{cb}}{V_{cs}V_{cb}} \mathcal{P}_{\pi^+} = \frac{f}{f_K} \mathcal{P}_{\pi^+} = 0.74 \pm 0.05; \quad (52)$$

where  $f = f_K = 0.34$  is the SU(3) breaking factor. Combining this result with

$$T = 2.7 \pm 0.6; \quad (53)$$

estimated from the measured branching ratio  $B(B^+ \rightarrow \pi^+ \pi^-) = (4.6 \pm 2.0) \times 10^{-6}$  and the assumed  $\text{Re}(C = T) = 0.1$  [37], they found the value of the ratio  $r$  [15]

$$r = \frac{P}{T} = 0.276 \pm 0.064; \quad (54)$$

From the values as given in Eqs.(46,51,54), one can see that the ratio  $r$  obtained by three different estimations are in good agreement within 1% error. From the analysis in this section and the estimations in next section where the newest data will be considered, we believe that it is reasonable to set  $r = 0.3 \pm 0.1$  in our calculations. In next section, we find that the measurements of relevant branching ratios prefer a ratio  $r$  larger than 0.16. In Belle's paper, they assumed that  $r = 0.3 \pm 0.15$  to draw the constraint on the CKM angle from their latest measurements of  $S$  and  $A$  [21].

Now we are ready to extract out  $\phi$  by comparing the theoretical prediction of  $S$  and  $A$  with the measured results. As discussed previously [16], there may exist some discrete ambiguities between  $\delta$  and  $\phi$  for the mapping of  $S$  and  $A$  onto the  $\delta$ - $\phi$  plane. We will consider the effects of such discrete ambiguity.

At first, the positiveness of the measured  $A$  at 2 level and the fact that  $\sin \phi > 0$  for  $0 < \phi < 180$  implies that  $\sin \delta$  should be negative, the range of  $0 < \delta < 180$  is therefore excluded under the parametrization of decay amplitude of  $B \rightarrow \pi^+ \pi^-$  as given in Eqs.(30,31). Consequently, only the range of  $180 < \delta < 360$  need to be considered here.

For the special case of  $\phi = 90$ , the discrete ambiguity between  $\delta$  and  $\phi$  disappears and the expressions of  $S$  and  $A$  can be rewritten as

$$S = \frac{\sin 2\delta}{1 + r^2}; \quad (55)$$

$$A = \frac{2r \sin \delta}{1 + r^2}; \quad (56)$$

which leads to the common allowed range of angle

$$98^\circ < \delta < 118^\circ \quad (57)$$

for  $S = 0.49 \pm 0.27$ ,  $A = 0.51 \pm 0.19$  and  $r = 0.30 \pm 0.10$ .

For an arbitrary value of  $\phi$  in the region of  $180 < \phi < 360$ , the constraint on the angle will change. In Fig. 3, we show the dependence of  $A$  for  $r = 0.3$  and  $\phi = 30$  (dots curve),  $60$  (dot-dashed curve),  $90$  (solid curve),  $120$  (short-dashed curve) and  $150$  (tiny-dashed curve), respectively. The band between two horizontal dots lines shows the allowed range  $0.32 < A^{\text{exp}} < 0.70$ . The vertical dots line refers to the physical limit  $\delta = 180$  with  $\phi = 23.6^\circ$ . It is easy to see from Fig. 3 that the regions allowed by the measured  $A$  alone at 1 level are

$$30^\circ < \delta < 150^\circ; \quad (58)$$

$$150^\circ < \delta < 30^\circ; \quad (59)$$

for  $r = 0.30$  and  $A = 0.51 \pm 0.19$ .

In Fig.4, we show the dependence of  $S$  for  $r = 0.3$  and  $\phi = 30$  (dots curve),  $60$  (dot-dashed curve),  $90$  (solid curve),  $120$  (short-dashed curve) and  $150$  (tiny-dashed curve), respectively. The band between two horizontal dots lines shows the measured value of  $S = 0.49 \pm 0.27$ . The vertical dots line shows the physical limit  $\delta = 180$  with  $\phi = 23.6^\circ$ . From this figure, we find that the range of  $82^\circ < \delta < 129^\circ$  is allowed by the measured  $S$  at 1 level.

Fig.5 shows the contour plots of the CP asymmetries  $S$  and  $A$  versus the strong phase and CKM angle  $\delta$  for  $r = 0.20$  (the dashed circles in (a)),  $0.30$  (the solid circles in (a)) and  $0.40$  (b), respectively. The regions inside each circle are allowed by both  $S^{\text{exp}} = 0.49 \pm 0.27$  and  $A^{\text{exp}} = 0.51 \pm 0.19$  for given  $r$ . The discrete ambiguity between  $\delta$  and  $\phi$  are also shown in Fig.5. For  $\phi = 90$ , such discrete ambiguity disappear. The horizontal short-dashed line is the physical limit  $\delta = 156.4^\circ$ , while the band between two horizontal dots lines shows the allowed region of  $30^\circ < \delta < 130^\circ$  from the global fit.

The constraint on the CKM angle  $\beta$  and the strong phase  $\delta$  can be read off directly from Fig.5. Numerically, the allowed regions for the CKM angle  $\beta$  and the strong phase  $\delta$  are

$$90^\circ < \beta < 121^\circ ; \quad 127^\circ < \delta < 55^\circ ; \quad (60)$$

for  $r = 0.2$ , and

$$83^\circ < \beta < 128^\circ ; \quad 150^\circ < \delta < 33^\circ ; \quad (61)$$

for  $r = 0.3$ , and finally

$$76^\circ < \beta < 135^\circ ; \quad 160^\circ < \delta < 26^\circ ; \quad (62)$$

$$148^\circ < \beta < 158^\circ ; \quad 135^\circ < \delta < 45^\circ ; \quad (63)$$

for  $r = 0.4$ . There is a twofold ambiguity for the determination of angle  $\beta$  for  $r = 0.4$ , but the second region of  $\beta$  in Eq. (63) is strongly disfavored by the global fit result as illustrated in Fig.5 and will be dropped.

Obviously, the constraints on  $\beta$  strongly depend on the value of  $r$ . In Fig.6 we draw the contour plots of the CP asymmetries  $S$  and  $A$  in the  $r$  plane for  $\delta = 60^\circ$  (short-dashed curves),  $90^\circ$  (solid curves) and  $120^\circ$  (dotted curves), respectively. The regions inside each semi-circle are allowed by both  $S^{\text{exp}} = 0.49 \pm 0.27$  and  $A^{\text{exp}} = 0.51 \pm 0.19$  (experimental allowed ranges when the FDG scaling factor is not considered). The upper short-dashed line shows the physical limit  $\beta = 156.4^\circ$ , the band between two horizontal dotted lines shows the global fit result. From this figure and the numerical calculations we find a lower limit on  $r$ ,

$$r \geq 0.16 \quad (64)$$

for the whole possible ranges of  $\beta$  and  $\delta$ , which agrees well with previous estimations.

In Ref. [21], based on their own newest measurement, Belle Collaboration presented the allowed region of  $\beta$  (at 95.5% C.L.)

$$78^\circ < \beta < 152^\circ \quad (65)$$

for  $\delta = 23.5^\circ$  and  $0.15 \leq r \leq 0.45$ .

In our analysis, we used the weighted average of BaBar and Belle's measurements of CP-violating asymmetries and  $r = 0.3 \pm 0.1$  as the experimental and theoretical input. Our result is in good agreement with Belle's constraint (65) where only their own measurement of  $S$  and  $A$  were used.

One can see from above analysis that if we take the average  $S = 0.49 \pm 0.27$  and  $A = 0.51 \pm 0.19$  as the experimental input, and use the theoretically fixed ratio  $r = 0.3 \pm 0.1$ , we find a strong constraint on  $\beta$ ,

$$76^\circ < \beta < 135^\circ \quad (66)$$

This range of  $\beta$  is well consistent with the global fit result [6,8,23]. On the other hand, the constraint on the strong phases  $\delta$  from the measured  $S$  and  $A$  is still rather weak.

As discussed in the introduction, the measurements of  $S$  and  $A$  as reported by BaBar and Belle Collaboration are not fully consistent. We should consider the case of using the weighted-average with the errors magnified by the PDG scaling factor, as already given in Eq.(7)

$$S = 0.49 \pm 0.61; A = +0.51 \pm 0.23; \quad (67)$$

In Fig.7, we draw the contour plots of the CP asymmetries  $S$  and  $A$  versus the strong phase  $\delta$  and the CKM angle  $\beta$  by using  $S = 0.49 \pm 0.61$  and  $A = 0.51 \pm 0.23$ . The allowed regions are then

$$78^\circ < \delta < 136^\circ; \quad 137^\circ < \beta < 43^\circ \quad (68)$$

for  $r = 0.2$ , and

$$71^\circ < \delta < 154^\circ; \quad 154^\circ < \beta < 26^\circ \quad (69)$$

for  $r = 0.3$ , and finally

$$64^\circ < \delta < 162^\circ; \quad 162^\circ < \beta < 18^\circ \quad (70)$$

for  $r = 0.4$ . It is easy to see from figures 5 and 7 that the constraints on  $\delta$  become less restrictive now.

In next section, we try to draw new constraints on the angle  $\beta$  and  $\delta$  from the measured CP-averaged branching ratios of  $B \rightarrow \pi^+ \pi^-$ ;  $\pi^+ \pi^0$  and  $B \rightarrow K^0 \pi^+$  decays.

#### IV. INFORMATION FROM MEASURED BRANCHING RATIOS

As listed in Table II, the CP-averaged branching ratios of  $B \rightarrow \pi^+ \pi^-$ ;  $\pi^+ \pi^0$  and  $B \rightarrow K^0 \pi^+$  decay modes have been measured with rather good precision. From these measured ratios one can infer that (a) the ratio of tree to penguin amplitudes  $r = |P|/|T|$ ; and (b) the constraint on the angle  $\delta$  and strong phase  $\delta$ . Of course, the information from measured  $B(B \rightarrow K)$  and  $B(B \rightarrow \pi)$  can be used as a crosscheck for the results obtained in the last section.

##### A. The measured branching ratios and the ratio $r$

In this paper, we use the following assumptions in addition to the SM [18]:

1. SU(2) isospin asymmetry of the strong interactions.
2. The breaking of SU(3) flavor symmetry of the strong interactions is described by the ratio of  $f_\pi/f_K$  with  $f_\pi = 133$  MeV and  $f_K = 158$  MeV as given in Table I.
3. Neglect of the suppressed annihilation diagrams and the electroweak penguin contributions.

4. Neglect of the penguin contributions which is proportional to  $V_{us}V_{ub}$  in the  $B^+ \rightarrow K^0 \pi^+$  decay amplitude.

Following Ref. [32], the flavor-SU(3) decomposition of  $B \rightarrow \pi \pi$ ;  $\pi^+ \pi^0$  and  $K^0 \pi^+$  decay amplitudes can be in general written as

$$A(B^+ \rightarrow \pi^+ \pi^0) = \frac{1}{\sqrt{2}} (T + C + P_{EW} + P_{EW}^C); \quad (71)$$

$$A(B^0 \rightarrow \pi^+ \pi^-) = T + P - \frac{2}{3} P_{EW}^C; \quad (72)$$

$$A(B^+ \rightarrow K^0 \pi^+) = P^0 - \frac{1}{3} P_{EW}^C; \quad (73)$$

where the unprimed amplitudes denote strangeness-preserving ( $\Delta S = 0$ )  $b \rightarrow d$  decays, the primed amplitudes denote strangeness changing ( $\Delta S = 1$ )  $b \rightarrow s$  decays. The amplitude  $T$  is color-favored tree amplitude,  $C$  is the color-suppressed tree amplitude,  $P$  and  $P^0$  are gluon penguin amplitudes, and  $P_{EW}$  and  $P_{EW}^C$  are the color-allowed and color-suppressed electroweak penguins (EWP) <sup>4</sup>. From previous studies [32,37,38], we get to know that

The electroweak penguin component in  $B^+ \rightarrow \pi^+ \pi^0$  decay (which is purely  $I = 2$ ) should be between  $O(10^{-2})$  and  $O(10^{-3})$  of the dominant  $T$  contribution [32], which is in agreement with Deshpande and He's estimation [38]:  $P_{EW} = T \times (1.6\% \times V_{td}/V_{ub})$ . For the contribution due to  $P_{EW}^C$ , it is in fact much smaller than that of  $P_{EW}$  because of further color-suppression. The EWP contributions to  $B^+ \rightarrow \pi^+ \pi^0$ ;  $\pi^+ \pi^-$  and  $K^0 \pi^+$  decays are therefore very small and can be neglected safely.

The effects of EWP amplitudes on the extraction of the CKM angle  $\alpha$  are at most of order  $10^{-2}$  and are negligible [32].

By employing the assumptions 1-4, one can find the constraint on the size of  $r$  from the measured CP-averaged branching ratios as listed in Table II. This is shown below.

#### B. Current estimations of $|T|/|C|$ and $|P|/|T|$

As discussed in last section, the ratio  $r = |P|/|T|$  can be estimated experimentally from the measured branching ratios of the tree dominated  $B \rightarrow \pi \pi$  decay and the pure penguin process  $B \rightarrow K^0 \pi^+$ . In this subsection, we update the estimation of the ratio  $r$  by considering the latest measurements of the two branching ratios.

When the electroweak penguin contribution is neglected, the  $B^+ \rightarrow \pi^+ \pi^0$  decay depends on tree amplitude  $T + C$  only. From the well measured branching ratio as given in Table II, one can determine the magnitude of  $|T + C|$ . If we quote all decay rates in units of ( $B$  branching ratio  $\times 10^6$ ) [15,19], the measured  $B \rightarrow \pi \pi$  branching ratio as given in Table II implies

---

<sup>4</sup>For a detailed discussion about the flavor SU(3) decomposition of two-body hadronic B meson decays, one can see Refs. [32,37] and references therein.

$$\begin{aligned}\overline{B}(B^+ \rightarrow \pi^+ \pi^0) &= \frac{1}{2} \overline{B}(B^+ \rightarrow \pi^+ \pi^0) + B(B^+ \rightarrow \pi^+ \pi^0) \\ &= \frac{1}{2} \overline{B}^+ \mathcal{T} + C \mathcal{J} = 5.3 \pm 0.8;\end{aligned}\quad (74)$$

We have to estimate the relative strength of  $\mathcal{T}$  and  $C$  contribution before we can extract  $\mathcal{T}$  from the measured branching ratio. In Ref. [37], the author assumed  $\text{Re}[C=\mathcal{T}] = 0.1$ . We here use the QCD factorization approach to estimate the value of  $\mathcal{J}=\mathcal{T}$ .

Under the QCD factorization approach, the decay amplitudes of  $B^+ \rightarrow \pi^+ \pi^0$  and  $B^+ \rightarrow K^0 \pi^+$  can be written as [35]

$$A(B^+ \rightarrow \pi^+ \pi^0) = i \frac{G_F}{2} (m_B^2 - m_\pi^2) F_0^{B\pi} (m_\pi^2) f_\pi V_{ub} V_{ud} [a_1 + a_2]; \quad (75)$$

where  $a_1$  and  $a_2$  describe the tree and the color-suppressed tree contributions, the small electroweak penguin has been neglected. Using the coefficients  $a_{1,2}$  at the NLO level as given in Ref. [35], we find numerically that

$$\mathcal{J}=\mathcal{T} \quad \mathcal{J}_2=a_1 \quad 0.10 \quad (76)$$

for  $m_b=2$  to  $2m_b$  with  $m_b = 4.6$  GeV. It is therefore reasonable to set

$$\mathcal{J}=\mathcal{T} \quad \mathcal{J} = 0.10^{+0.10}_{-0.05} \quad (77)$$

in our analysis. From Eqs.(74) and (77), we then find that

$$\overline{B}^+ \rightarrow \pi^+ \pi^0 = 2.8 \pm 0.2 (\text{Br}) \pm 0.2 (\mathcal{J}=\mathcal{T}) = 2.8 \pm 0.3 \quad (78)$$

for  $B(B^+ \rightarrow \pi^+ \pi^0) = (5.3 \pm 0.8) \times 10^{-6}$  and  $\pi^+ \pi^0 = 1.083 \pm 0.017$  [23]. This estimation of  $\mathcal{T} \rightarrow \pi^0$  agrees well with previous results  $\mathcal{T} \mathcal{J} = 2.7 \pm 0.6$  [19,37] but with smaller error due to the improvement of the data. From the assumption of the isospin symmetry of strong interaction, we have

$$\mathcal{T}^+ \rightarrow \pi^+ \mathcal{J} = \mathcal{T}^+ \rightarrow \pi^0 \mathcal{J} \quad (79)$$

For the sake of simplicity, we use terms  $\mathcal{T} \mathcal{J}$  and  $\mathcal{P} \mathcal{J}$  to denote  $\mathcal{T}^+ \rightarrow \pi^+ \mathcal{J}$  and  $\mathcal{P}^+ \rightarrow \pi^+ \mathcal{J}$  without further specification.

As discussed in last section, the strangeness-changing QCD penguin amplitude  $P^0 = P_K$  can be determined from the measured branching ratio  $\overline{B}(B^+ \rightarrow K^0 \pi^+)$  as given in Table II. In units of  $B$  branching ratio  $10^{-6}$ , we find

$$\overline{B}(B^+ \rightarrow K^0 \pi^+) = \frac{1}{2} \mathcal{P}_K \mathcal{J} = 19.7 \pm 1.5; \quad (80)$$

which leads to

$$\mathcal{P}_K \mathcal{J} = 4.3 \pm 0.2; \quad (81)$$

Using Gronau and Rosner convention [15] to define  $P$ , we find numerically that

$$\mathcal{P}_j = \frac{f}{f_K} \mathcal{P}_K \quad j = 0.80 \quad 0.04 \quad (82)$$

for  $f = 0.133 \text{ GeV}$  and  $f_K = 0.158 \text{ GeV}$ , which leads to the value

$$r = \mathcal{P} = T \quad j = 0.29 \quad 0.04 \quad (83)$$

for  $T = 2.8 \quad 0.3$  as given in Eq.(78).

Using the Luo and Rosner convention [19] to define  $\mathcal{P}$ , we find numerically that

$$\mathcal{P}_j = \mathcal{P}_1 \quad i \quad \mathcal{P}_K \quad j = 0.81 \quad 0.19 \quad (84)$$

for  $\mathcal{P} = 0.2196 \quad 0.0026$ ,  $\mathcal{P} = 0.22 \quad 0.10$  and  $\mathcal{P} = 0.35 \quad 0.05$  as given in Ref. [23]. The ratio  $r$  therefore takes the value of

$$r = \mathcal{P} = T \quad j = 0.29 \quad 0.07 \quad (85)$$

for  $T = 2.8 \quad 0.3$  as given in Eq.(78).

The ratios  $r$  in Eqs.(83) and (85) agree very well with those given in previous papers [15,19,35], but with smaller errors because of the improvement of the data. We believe that it is reasonable and conservative to set  $r = 0.3 \quad 0.1$  in our calculations.

#### C. Constraint on $\alpha$ and $\beta$ from measured branching ratios

Using the expressions of the decay amplitudes as given in Eqs.(30,31), the CP-averaged branching ratio of  $B^0 \rightarrow \pi^+ \pi^-$  decay can be written as

$$\overline{\mathcal{B}}(B^0 \rightarrow \pi^+ \pi^-) = \mathcal{T}^2 + \mathcal{P}^2 - 2\mathcal{T}\mathcal{P}\cos\alpha\cos\beta : \quad (86)$$

The world average of experimental measurements (in units of  $B$  branching ratio  $10^6$ ) implies

$$\overline{\mathcal{B}}(B^0 \rightarrow \pi^+ \pi^-) = \mathcal{T}^2 + \mathcal{P}^2 - 2\mathcal{T}\mathcal{P}\cos\alpha\cos\beta = 4.6 \quad 0.4 : \quad (87)$$

It is easy to find that

$$\mathcal{T}^2 + \mathcal{P}^2 = 8.5 \quad 1.3 > 4.6 \quad 0.4 \quad (88)$$

for  $\mathcal{T} = 2.8 \quad 0.3$  and  $\mathcal{P} = 0.81 \quad 0.19$ . In other words, the tree and penguin amplitudes in  $B^0 \rightarrow \pi^+ \pi^-$  decay are indeed interfering destructively at  $2.6$  level. Consequently,  $\cos\alpha$  and  $\cos\beta$  in Eq.(87) should have the same sign. By scanning the whole ranges of  $\mathcal{T} = 2.8 \quad 0.3$ ,  $\mathcal{P} = 0.81 \quad 0.19$  and  $\overline{\mathcal{B}}(B^0 \rightarrow \pi^+ \pi^-) = 4.6 \quad 0.4$ , we find the lower limit

$$\cos\alpha\cos\beta = \frac{\mathcal{T}^2 + \mathcal{P}^2 - (4.6 \quad 0.4)}{2\mathcal{T}\mathcal{P}} \geq 0.45; \quad (89)$$

and more specially,

$$j \cos j = 0.45; \quad (90)$$

$$j \cos j = 0.45: \quad (91)$$

The minimum value of  $\cos \cos = 0.45$  corresponds to the choice of  $\mathcal{T} j = 2.5; \mathcal{P} j = 1.0$  (i.e.  $r = \mathcal{P} = \mathcal{T} j = 0.4$ ) and  $\overline{B}(B^0 \rightarrow \pi^+ \pi^-) = 5.0$ .

Within the physical ranges of  $0 < \alpha < 180$  and  $180 < \beta < 360$ , the inequality (89) leads to two sets of solutions,

$$\text{I: } 63 < \alpha < 117; \quad 0 < \beta < 63; \quad (92)$$

$$\text{II: } 180 < \alpha < 227; \quad 117 < \beta < 180: \quad (93)$$

It is easy to see that the regions

$$63 < \alpha < 117; \quad 117 < \beta < 63; \quad (94)$$

are excluded, which is a new and important information obtained from the measurements of the branching ratios of  $B \rightarrow \pi^+ \pi^-$ ;  $B \rightarrow \pi^0 \pi^0$  and  $B \rightarrow K^0 \pi^+$  decays. Further improvement of the data will help us to narrow the allowed ranges for both  $\alpha$  and  $\beta$ . Considering the direct measurement of the angle  $\alpha$  and the bounds on the angle  $\beta$  from global fit, the case of  $\alpha < 63$  is strongly disfavored, while the range of

$$117 < \alpha < 156.4 \quad (95)$$

is still allowed by direct measurement of the angle  $\alpha$  and the data of relevant branching ratios.

In Fig.8 we draw the contour plots of Eq. (89) in the  $\alpha$ - $\beta$  plane. The two regions at the upper-left and lower-right corner bounded by solid curves are still allowed by the constraint  $\cos \cos = 0.45$ . One can see from Fig.8 that the first solution (i.e. the lower-right corner region) as specified in Eq.(92) is strongly disfavored by the global fit result,  $70 < \alpha < 130$ , as illustrated by the band between two dots lines in figure 8.

#### D. Combined result

Now we combine the constraints on the CKM angle  $\alpha$  and strong phase  $\delta$  from the experimental measurements studied in this paper.

Fig.9 is the combination of Fig. 5b and Fig. 8 for  $r = 0.4$ . The upper dot-dashed line shows the direct physical limit of  $\alpha = 156.4$  from the BaBar and Belle's measurements of  $\sin 2\alpha$ . The regions inside the solid circles are allowed by both  $S^{\text{exp}} = 0.49 \pm 0.27$  and  $A^{\text{exp}} = 0.51 \pm 0.19$  for  $r = 0.4$ . The regions at the upper-left and lower-right corner bounded by short-dashed curves are allowed by the constraint  $\cos \cos = 0.45$  for  $r = 0.4$ . The commonly allowed region can be seen from Fig. 9, and the combined constraints on the CKM angle  $\alpha$  and the strong phase  $\delta$  are

$$117 < \alpha < 135; \quad (96)$$

$$160 < \delta < 132: \quad (97)$$



The constraint on  $\delta$  is in very good agreement with that from global fit, illustrated by the horizontal band between two dots lines,  $70^\circ < \delta < 130^\circ$ , and will be improved along with progress of experimental measurements. The lower limit of  $\delta = 117^\circ$  is much stronger than the limits obtained before. The constraint on the strong phase  $\phi$ , however, depends on the convention to choose the relative phase between the tree and penguin amplitudes.

From Fig.9, one can also see that the discrete ambiguity between  $\delta$  and  $\delta + 180^\circ$  is resolved by the inclusion of the three measured branching ratios.

Fig.10 is the combination of Fig. 7b and Fig. 8 for  $r = 0.4$ . The lower and upper limit on  $\delta$  are dominated by the constraint from the measured branching ratios and by the direct physical limit  $156.4^\circ$  respectively, while the constraint on  $\delta$  from the measured  $S$  and  $A$  becomes rather weak when one uses the enlarged errors as the 1 $\sigma$  experimental errors. The allowed regions of the angle  $\delta$  and  $\phi$  can then be read from Fig.10 directly,

$$117^\circ < \delta < 156.4^\circ; \quad (98)$$

$$162^\circ < \phi < 132^\circ; \quad (99)$$

The experimental errors of the measured branching ratios of  $B \rightarrow \pi^+ \pi^-$ ;  $\pi^0 \pi^0$  and  $K^0 \pi^+$  as given in Table II are around 10% now. The errors of the measured  $S$  and  $A$  as reported by BaBar and Belle Collaborations are still large. By comparing the figures 9 and 10, one can see clearly that the improvement of the experimental measurements of  $S$  and  $A$  is very important for us to determine the CKM angle  $\delta$  reliably. Besides the error in estimating the magnitude of  $|T|$ , the main theoretical error in our method may also come from the neglecting of annihilation type diagrams, which was shown not very small in some model calculations [39].

## V. SUMMARY

In this paper, we study and try to find constraints on the CKM angle  $\delta$  and the strong phase  $\phi$  from the experimental measurements of  $\sin(2\delta)$ , the CP-violating asymmetries of  $B \rightarrow \pi^+ \pi^-$  decay, the CP-averaged branching ratios of  $B \rightarrow \pi^+ \pi^-$ ;  $\pi^0 \pi^0$  and  $K^0 \pi^+$  decays.

In Section II, we give a brief review about the CKM angles and quote the constraints on these angles obtained from the global fit [8,29]. From the measured  $\sin(2\delta)$  [2,4], the direct physical upper limit on  $\delta$  is  $156.4^\circ$  for  $r = 23.6\%$ .

In section III, we draw constraints on  $\delta$  and  $\phi$  from the measured CP-violating asymmetries of  $S$  and  $A$ . By taking the weighted-average of BABAR and Belle's measurements as the experimental input, we found the following constraints

$$76^\circ < \delta < 135^\circ; \quad 160^\circ < \phi < 26^\circ \quad (100)$$

for  $S = 0.49 \pm 0.27$ ,  $A = +0.51 \pm 0.19$  and  $r = 0.3 \pm 0.1$ , as shown in Fig.5, and

$$64^\circ < \delta < 162^\circ; \quad 162^\circ < \phi < 18^\circ \quad (101)$$

for  $S = 0.49 \pm 0.61$ ,  $A = +0.51 \pm 0.23$  and  $r = 0.3 \pm 0.1$ , as shown in Fig.7.

In section IV, we draw constraints on  $\delta$  and  $\phi$  from the measured CP-averaged branching ratios of  $B \rightarrow \pi^+ \pi^-$ ;  $\pi^0 \pi^0$  and  $B \rightarrow K^0 \pi^+$  decays as given in Table II. In the analysis,

SU(2) isospin symmetry and other three assumptions are employed. From the measured decay rates of  $B^+ \rightarrow \pi^+ \pi^0$  and  $B^+ \rightarrow K^0 \pi^+$ , one can determine the tree and penguin amplitudes of  $B \rightarrow \pi^+ \pi^0$  decay:  $|T| = 2.8 \pm 0.3$ , while  $|P| = 0.80 \pm 0.04$  in GR convention [15] and  $|P| = 0.81 \pm 0.19$  in LR convention [19]. The destructive interference between the tree and penguin amplitudes of  $B \rightarrow \pi^+ \pi^0$  decay is then established at 2.6 level. The regions

$$63^\circ < \alpha < 117^\circ; \quad 117^\circ < \alpha < 63^\circ \quad (102)$$

are excluded by the inequality  $\cos \alpha \cos \beta > 0.45$  as given in Eq.(89), which is a new and important information from the measurements of the relevant branching ratios.

The combined constraints on the CKM angle  $\alpha$  and strong phase  $\delta$  have been given in Eqs.(96-97), as illustrated in Figs.9 and 10. The common allowed regions for  $\alpha$  and  $\delta$  are

$$117^\circ < \alpha < 135^\circ; \quad 160^\circ < \delta < 132^\circ; \quad (103)$$

for  $S = 0.49 \pm 0.27$ ,  $A = +0.51 \pm 0.19$  and  $r = 0.4$ , while

$$117^\circ < \alpha < 156.4^\circ; \quad 162^\circ < \delta < 132^\circ; \quad (104)$$

for  $S = 0.49 \pm 0.61$ ,  $A = +0.51 \pm 0.23$  and  $r = 0.4$ .

In short, we are able to draw strong constraint on the CKM angle  $\alpha$  from currently available experimental measurements considered in this paper. The new lower limit on the angle  $\alpha$  is dominated by the inequality  $\cos \alpha \cos \beta > 0.45$  and much stronger than those obtained before. In the SM, the measured value of the angle  $\alpha$  gives a physical upper limit on the CKM angle  $\alpha$ . The measured CP-violating asymmetries  $S$  and  $A$  can lead to a strong upper limit on  $\alpha$  if we take  $S = 0.49 \pm 0.27$  and  $A = 0.51 \pm 0.19$  as the experimental input. If we consider the enlarged errors of  $S$  and  $A$ , however, the corresponding upper limit becomes weak. The constraints from different sources are complementary to pin down the allowed region of  $\alpha$ . Further improvement of the data will help us to determine  $\alpha$  with a good precision.

#### ACKNOWLEDGMENTS

Z.J.Xiao and L.B.Guo acknowledge the support by the National Natural Science Foundation of China under Grants No.10075013 and 10275035, and by the Research Foundation of Nanjing Normal University under Grant No.214080A916. C.D.Lu acknowledges the support by National Science Foundation of China under Grants No.90103013 and 10135060.

## REFERENCES

- [1] BaBar Collaboration, B. Aubert et al., Phys. Rev. Lett. 87, 091801 (2001); BaBar Collaboration, B. Aubert et al., Phys. Rev. D 66, 032003 (2002).
- [2] BaBar Collaboration, B. Aubert et al., Phys. Rev. Lett. 89, 201802 (2002).
- [3] Belle Collaboration, K. Abe et al., Phys. Rev. Lett. 87, 091802 (2001); Belle Collaboration, K. Abe et al., Phys. Rev. D 66, 032007 (2002).
- [4] Belle Collaboration, K. Abe et al., Phys. Rev. D 66, 071102 (2002).
- [5] Y. Nir, plenary talk presented at ICHEP2002, Amsterdam, 21-24 July, 2002; hep-ph/0208080;
- [6] A. Hocker, H. Lacker, S. Laplace and F. Le Diberder, Eur. Phys. J. C 21, 225 (2001); A. F. Falk, Flavor physics and the CKM matrix: An overview, hep-ph/0201094.
- [7] X. G. He, Y. K. Hsiao, J. Q. Shi, Y. L. Wu and Y. F. Zhou, Phys. Rev. D 64, 034002 (2001).
- [8] For details of extraction of the CKM angles, see M. Battaglia et al., The CKM matrix and the unitarity triangle, to appear as a CERN Report, eds. M. Battaglia, A. J. Buras, P. Gambino, A. Stocchi (2003), hep-ph/0304132.
- [9] R. Fleischer, and J. Matias, Phys. Rev. D 66, 054009 (2002).
- [10] Y. Grossman and H. R. Quinn, Phys. Rev. D 56, 7259 (1997); J. Charles et al., Phys. Lett. B 425, 375 (1998); B. Kayser and D. London, Phys. Rev. D 61, 116012 (2000); H. R. Quinn et al., Phys. Rev. Lett. 85, 5284 (2000).
- [11] R. Fleischer, Phys. Lett. B 365, 399 (1996); Phys. Lett. B 459, 306 (1999), Eur. Phys. J. C 10, 299 (1999); R. Fleischer, and T. Mannel, Phys. Rev. D 57, 2752 (1998); M. Gronau and J. L. Rosner, Phys. Rev. D 57, 6843 (1998).
- [12] R. Fleischer, Eur. Phys. J. C 6, 451 (1999); Eur. Phys. J. C 16, 87 (2000); M. Neubert, and J. L. Rosner, Phys. Lett. B 441, 403 (1998); A. J. Buras, and R. Fleischer, Eur. Phys. J. C 11, 93 (1999); Eur. Phys. J. C 16, 97 (2000).
- [13] For more details about the extraction of  $\alpha$  from  $B \rightarrow \pi^0 \pi^0$  and  $K$  decays, see R. Fleischer, Phys. Rep. 370, 537 (2002); R. Fleischer, hep-ph/0208083.
- [14] Z. J. Xiao and M. P. Zhang, Phys. Rev. D 65, 114017 (2002).
- [15] M. Gronau and J. L. Rosner, Phys. Rev. D 65, 013004 (2002).
- [16] M. Gronau and J. Rosner, Phys. Rev. D 65, 093012 (2002).
- [17] C. D. Lu and Z. J. Xiao, Phys. Rev. D 66, 074011 (2002).
- [18] J. Charles, Phys. Rev. D 59, 054007 (1999).
- [19] Z. Luo and J. L. Rosner, Phys. Rev. D 65, 054027 (2002).
- [20] BaBar Collaboration, B. Aubert et al., Phys. Rev. Lett. 89, 281802 (2002).
- [21] Belle Collaboration, K. Abe et al., Evidence for CP-violating asymmetries in  $B^0 \rightarrow \pi^+ \pi^-$  decays and constraints on the CKM angle  $\alpha$ , hep-ex/0301032.
- [22] Belle Collaboration, K. Abe et al., Phys. Rev. Lett. 89, 071801 (2002).
- [23] Particle Data group, K. Hagiwara et al., Phys. Rev. D 66, 010001-1 (2002).
- [24] A. Bomheim et al., CLEO Collab., Measurements of charmless hadronic two-body B meson decays and the ratio  $B(B \rightarrow D^0 K)/B(B \rightarrow D^0 \pi)$ ; hep-ex/0302026.
- [25] B. Aubert et al., BaBar Collaboration, quoted by S. Playfer at LHCb Workshop, CERN, Feb. 2003. B. Aubert et al., BaBar Collaboration, Observation of the decay  $B^0 \rightarrow \pi^0 \pi^0$ , study of  $B^0 \rightarrow K^0 \pi^0$ , and search for  $B^0 \rightarrow \pi^0 \pi^0 \pi^0$ , SLAC-PUB-9683, hep-ex/0303028.
- [26] T. Tomura, Belle Collaboration, Rare hadronic B decays and direct CPV, talk presented

- at 28 Rencontre De Moriond: EW Inter. and Unified Theories, Les Arcs, France, Mar. 15–22, 2003;
- [27] M. Kobayashi and T. Maskawa, *Prog. Theor. Phys.* 49, 652 (1973).
  - [28] L. Wolfenstein, *Phys. Rev. Lett.* 51, 1945 (1983).
  - [29] R. Fleischer, *hep-ph/0305267*.
  - [30] D. London, N. Sinha, and R. Sinha, *Phys. Rev. D* 60, 074020 (1999).
  - [31] I.I. Bigi and A.I. Sanda, *CP violation*, Cambridge University Press, Cambridge, 2000.
  - [32] M. Gronau, O.F. Hernandez, D. London and J.L. Rosner, *Phys. Rev. D* 50, 4529 (1994); *Phys. Rev. D* 52, 6356 (1995); *Phys. Rev. D* 52, 6374 (1995); J. Silva and L. Wolfenstein, *Phys. Rev. D* 49, 1151 (1994).
  - [33] M. Gronau and D. London, *Phys. Rev. Lett.* 65, 3381 (1990).
  - [34] M. Beneke, G. Buchalla, M. Neubert and C.T. Sachrajda, *Phys. Rev. Lett.* 83, 1914 (1999).
  - [35] M. Beneke, G. Buchalla, M. Neubert and C.T. Sachrajda, *Nucl. Phys. B* 606, 245 (2001).
  - [36] T. Yoshikawa, *hep-ph/0304038*.
  - [37] J.L. Rosner, *Nucl. Instrum. Meth. A* 462, 44 (2001).
  - [38] N.G. Deshpande and X.-G. He, *Phys. Rev. Lett.* 74, 26 (1995).
  - [39] C.-D. Lu, K. Ukai and M.-Z. Yang, *Phys. Rev. D* 63, 074009 (2001); C.D. Lu, *Eur. Phys. J. C* 24, 121 (2002); C.-D. Lu and K. Ukai, *hep-ph/0210206*.

# TABLES

TABLE I. Values of the input parameters used in the numerical calculations. Most of them are quoted from PDG 2002 [23]. All masses are in the unit of GeV.

| $\mathcal{V}_{us} =$ |        | $\mathcal{V}_{cb} =$ |      | $\mathcal{V}_{ub} =$ |      | $\mathcal{V}_{td} =$ |           | $V_{tb}$    |      |           |   |
|----------------------|--------|----------------------|------|----------------------|------|----------------------|-----------|-------------|------|-----------|---|
| 0.2196               | 0.0026 | (41.2                | 2.0) | $10^{-3}$            | (3.6 | 0.7)                 | $10^{-3}$ | (7.9        | 1.5) | $10^{-3}$ | 1 |
| $m_W$                |        | $m_t$                |      | $m_b^{\text{pole}}$  |      | $m_{B_d}$            |           | $m_{B_s}$   |      |           |   |
| 80.42                |        | 175                  |      | 4.80 0.15            |      | 5.279                |           | 5.369       |      |           |   |
| $f$                  |        | $f_K$                |      | 0                    |      | +                    |           | + = 0       |      |           |   |
| 0.133                |        | 0.158                |      | 1.542ps              |      | 1.674ps              |           | 1.083 0.017 |      |           |   |

TABLE II. Experimental measurements of the CP-averaged branching ratios for  $B \rightarrow \pi^+ \pi^-$ ;  $B \rightarrow \pi^0 \pi^0$  and  $K \rightarrow \pi^+ \pi^-$  decays (in units of 10<sup>-6</sup>) as reported by CLEO [24], BaBar [25] and Belle Collaboration [26]. The numbers in last column are the weighted average.

| Channel                     | CLEO                         | BaBar                        | Belle                  | Average        |
|-----------------------------|------------------------------|------------------------------|------------------------|----------------|
| $\pi^+ \pi^-$               | $4.5^{+1.4+0.5}_{-1.2-0.4}$  | $4.7 \pm 0.6 \pm 0.2$        | $4.4 \pm 0.6 \pm 0.3$  | $4.6 \pm 0.4$  |
| $\pi^+ \pi^0$               | $4.6^{+1.8+0.6}_{-1.6-0.7}$  | $5.5^{+1.0}_{-0.9} \pm 0.6$  | $5.3 \pm 1.3 \pm 0.5$  | $5.3 \pm 0.8$  |
| $K \rightarrow \pi^+ \pi^-$ | $18.8^{+3.7+2.1}_{-3.3-1.8}$ | $17.5^{+1.8}_{-1.7} \pm 1.3$ | $22.0 \pm 1.9 \pm 1.1$ | $19.7 \pm 1.5$ |

# FIGURES

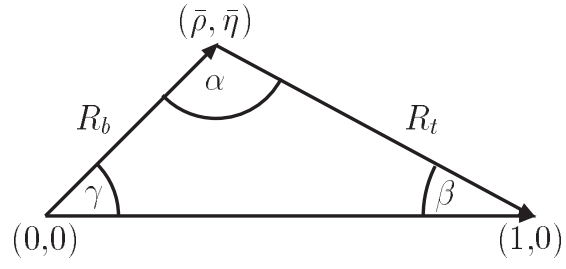


FIG .1. Unitarity triangle in  $\bar{\rho} - \bar{\eta}$  plane, corresponding to the  $b \rightarrow d$  transition.

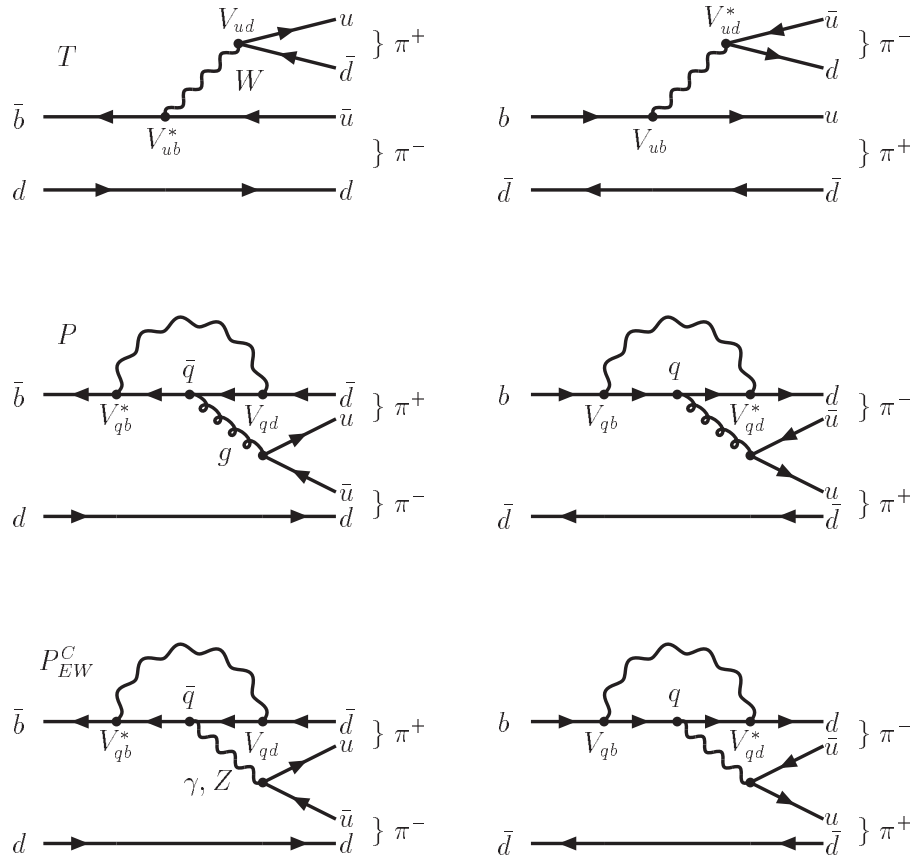


FIG. 2. The tree (T), QCD penguin (P) and color-suppressed electroweak penguin ( $P_{EW}^C$ ) diagrams with  $q = u, c, t$ , contributing to the  $B_d^0 \rightarrow \pi^+ \pi^-$  decays.

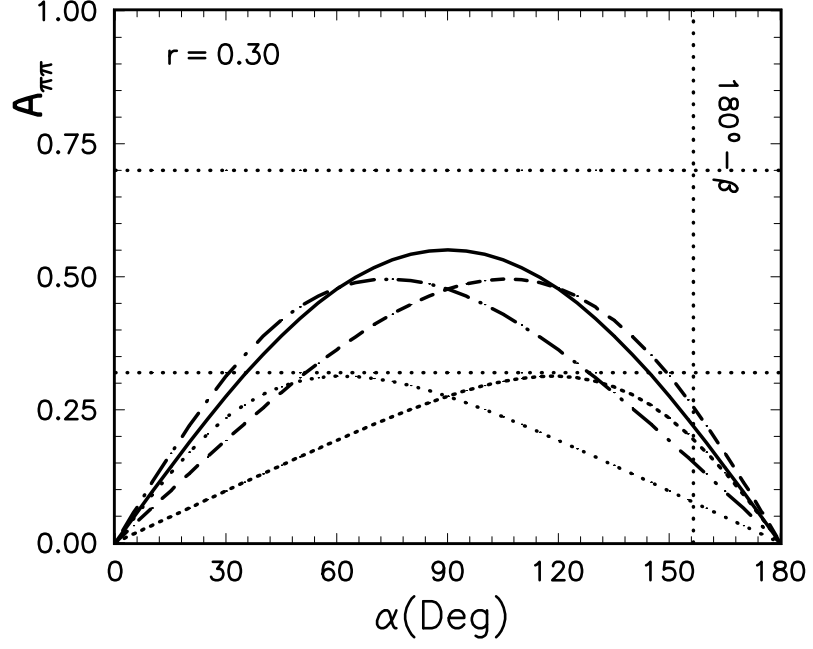


FIG. 3. Plots of  $A_{\pi\pi}$  vs angle  $\alpha$  for  $r = 0.30$ . The five curves correspond to  $\beta = 30$  (dotted curve),  $60$  (dot-dashed curve),  $90$  (solid curve),  $120$  (short-dashed curve) and  $150$  (tiny-dashed curve), respectively. The band between two horizontal dotted lines shows the allowed range  $0.32 \leq A_{\pi\pi}^{\text{exp}} \leq 0.70$  at  $1\sigma$  level. The vertical dotted line refers to the physical limit  $156.4^\circ$ .



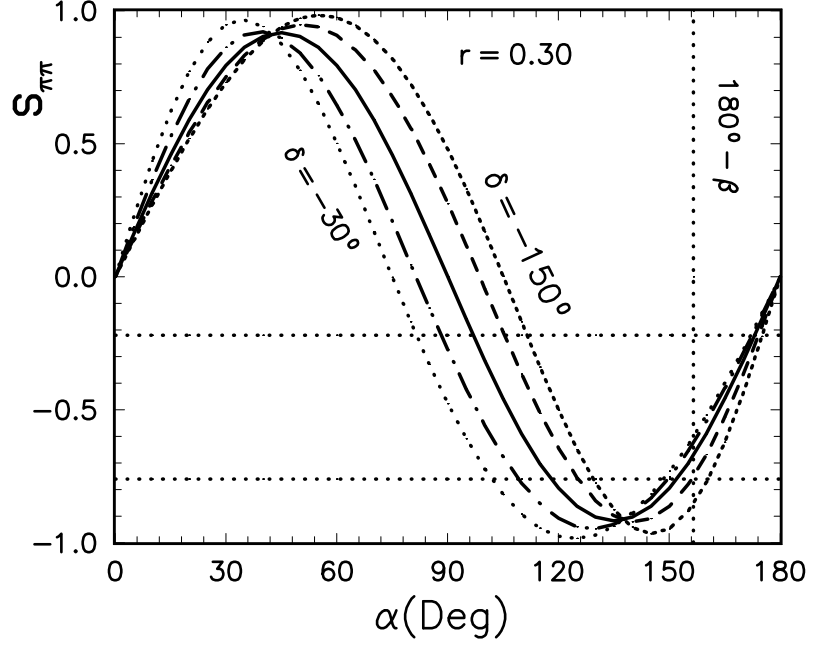


FIG. 4. Plots of  $S_{\pi\pi}$  vs angle for  $r = 0.30$  and  $150^\circ \leq \delta \leq 180^\circ$ . From the left to the right the five curves correspond to  $\delta = 30^\circ, 60^\circ, 90^\circ, 120^\circ$  and  $150^\circ$ , respectively. The band between two horizontal dots lines shows the allowed range  $0.76 \leq S_{\pi\pi}^{\text{exp}} \leq 0.22$  at 1 level. The vertical dots line refers to the physical limit  $156.4^\circ$ .

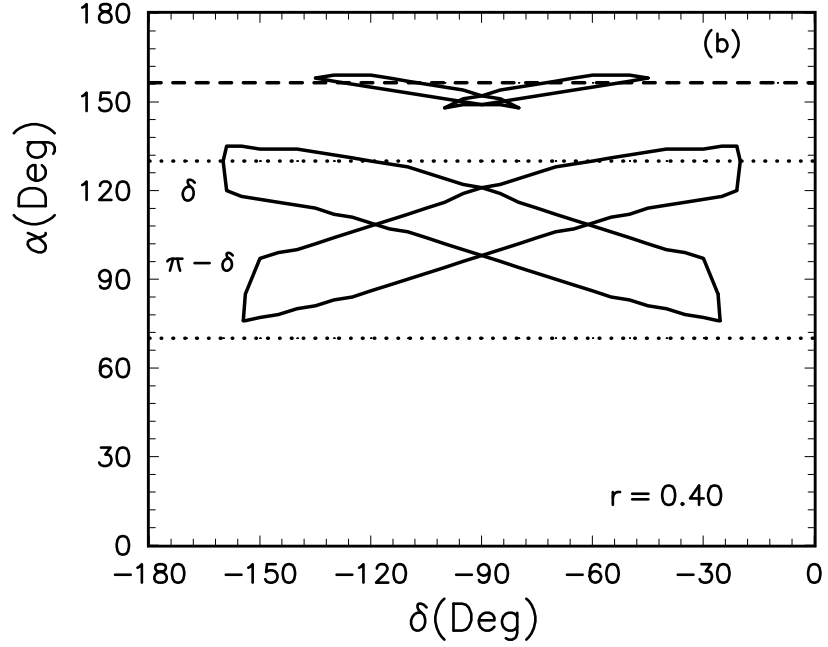
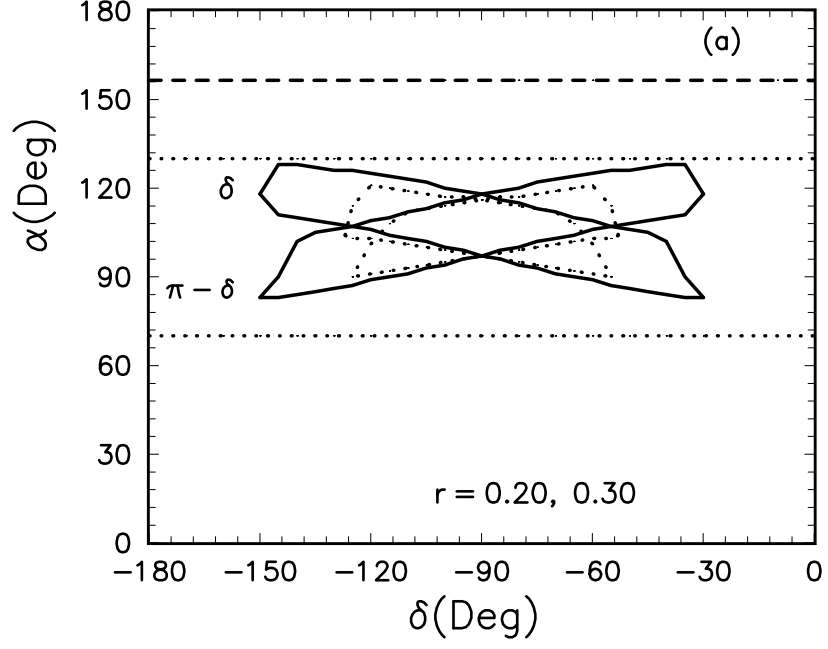


FIG. 5. Contour plots of the asymmetries  $S$  and  $A$  versus the CKM angle  $\delta$  and the strong phase  $\alpha$  for  $r = 0.2$  (the dots circles in (a)),  $0.3$  (the solid circles in (a)), and  $0.4$  (b), respectively. The upper short-dashed line shows the physical upper limit, while the band between two horizontal dots lines shows the global fit result:  $70^\circ - 130^\circ$ .

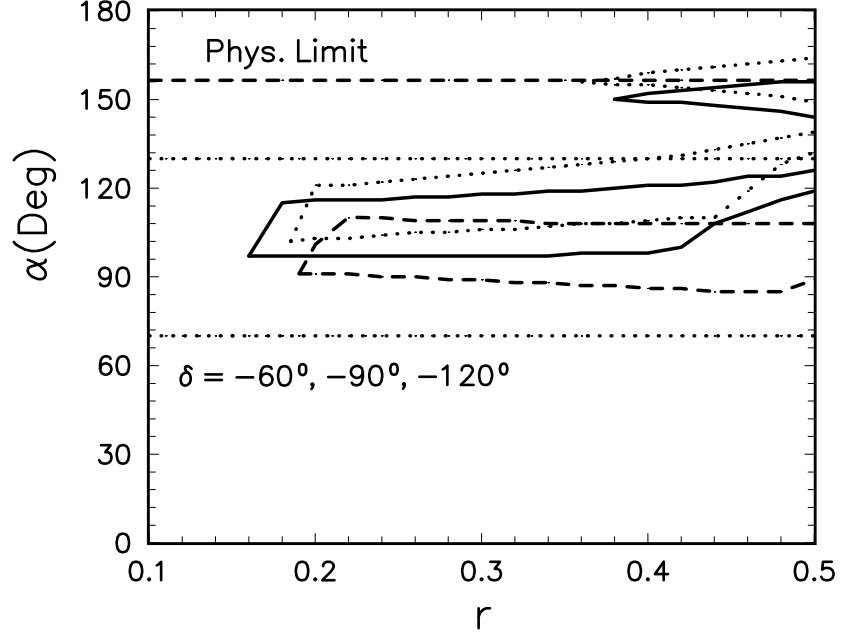


FIG. 6. Contour plots of the asymmetries  $S$  and  $A$  versus the CKM angle  $\alpha$  and the ratio  $r = P/T$  for  $\delta = -60^\circ$  (dots curves),  $-90^\circ$  (solid curves) and  $-120^\circ$  (short-dashed curves), respectively. The regions inside the semi-closed curves are allowed by the data. The upper short-dashed line shows the physical limit  $156.4^\circ$ , while the band between two horizontal dots lines shows the global  $\tau$  result:  $70^\circ - 130^\circ$ .

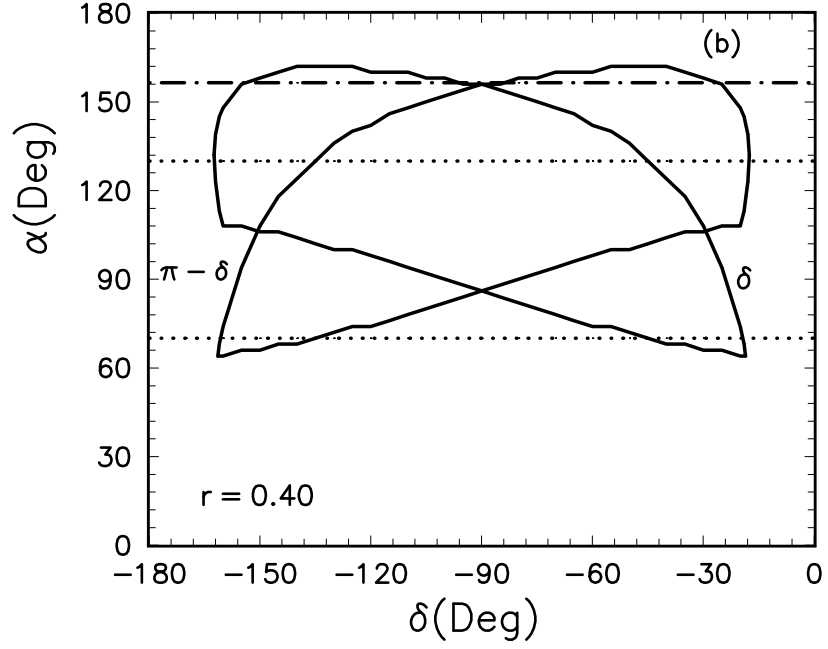
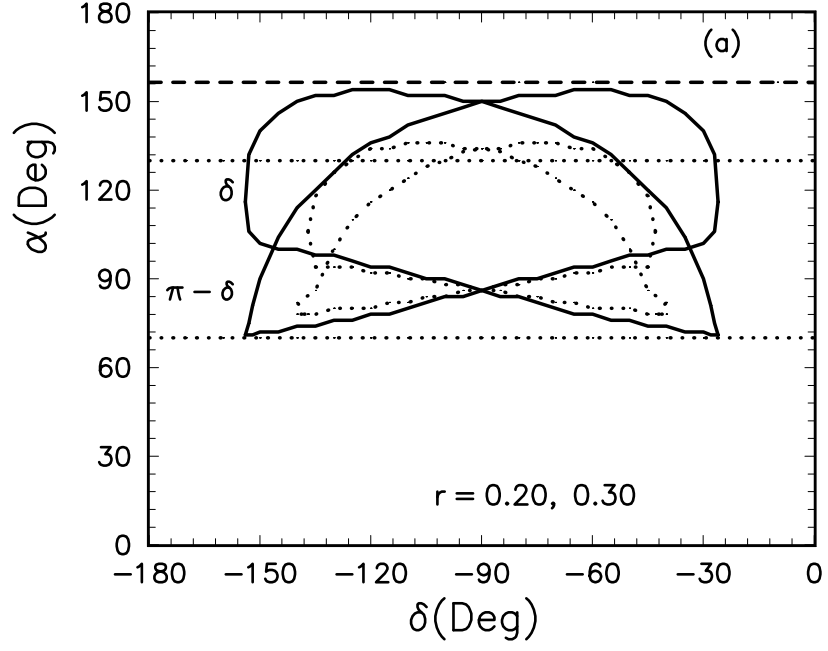


FIG. 7. The same as Fig. 5, but using  $S = 0.49 - 0.61$  and  $A = 0.51 - 0.23$  as the experimental input.

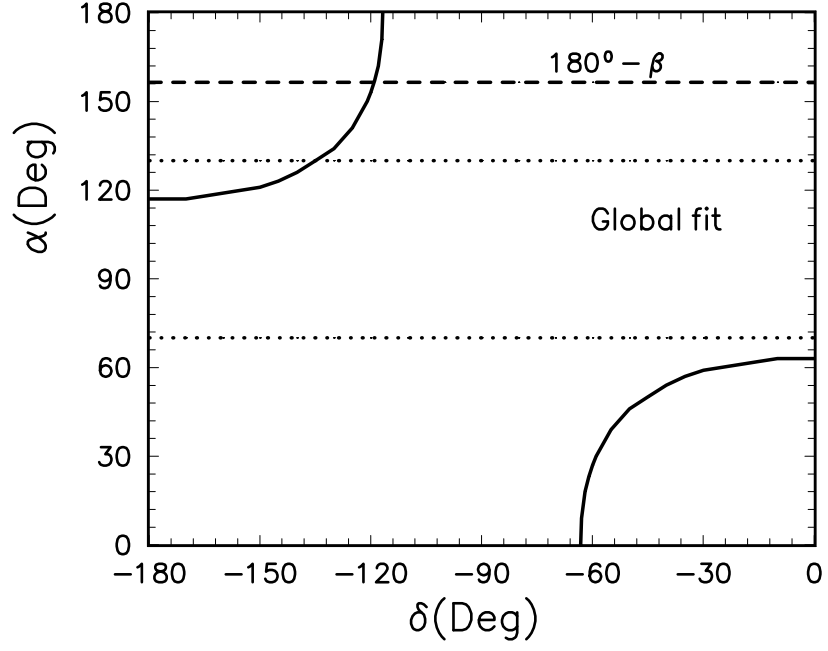


FIG. 8. Contour plots of the branching ratio  $\overline{B}(B \rightarrow \pi^+ \pi^-)$  versus the CKM angle  $\delta$  and the strong phase  $\alpha$ . The regions at the upper-left and the lower-right corner bounded by solid curves are still allowed by the inequality  $\cos \delta \cos \alpha \geq 0.45$ .

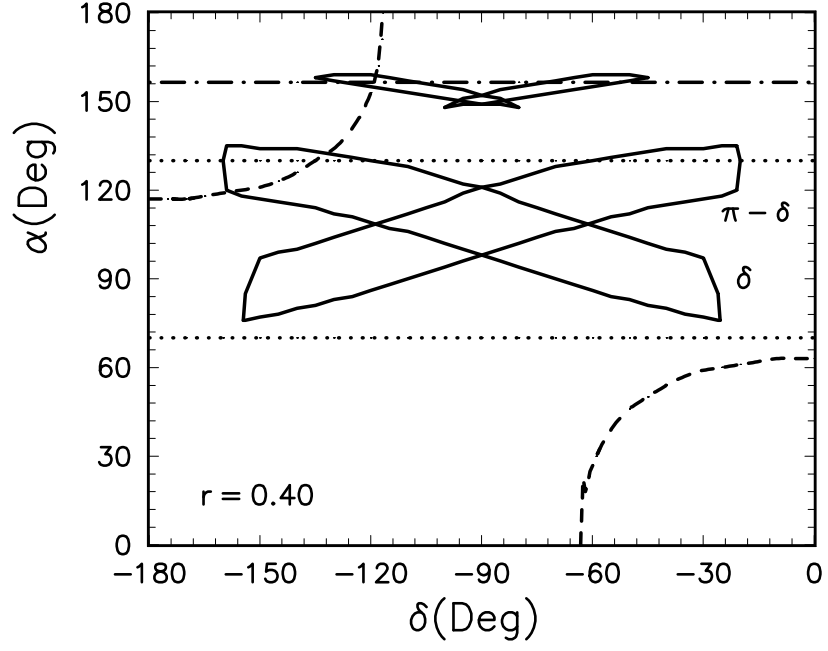


FIG. 9. The combined constraints on  $\alpha$  and  $\delta$  for  $r = 0.4$  and taking  $S = 0.49 \pm 0.27$ ,  $A = 0.51 \pm 0.19$  as the experimental input. For details see text.

